Active fault-tolerant control of a Quadrotor UAV against actuator faults based on backstepping technique and adaptive observer

Abderrahim EZZARA[1], Ahmed Youssef OUADINE [2], Hassan AYAD[1]

[1]LSEET, Department of Applied Physics, Faculty of Science and Technology Gueliz, Marrakech, 40000, Morocco

ezzara.abderrahim@gmail.com (*Corresponding author*) ayad.ha@gmail.com

[2] Ecole Royale de l'Air

a.y.ouadine@gmail.com

Abstract: This paper addresses the stabilization problem of an underactuated quadrotor UAV system in presence of actuator faults. First, a dynamic model of the quadcopter was established using a Lagrange approach. High-order non-holonomic constraints as well as different physical phenomena that can influence the dynamics of the structure have been taken into account. Then, for actuator faults, a new active fault tolerance strategy based on a backtracking approach and an adaptive observer is developed. The simulation results obtained illustrate the ability of the proposed control strategy to maintain performance and preserve stability in the event of actuator failure.

Introduction

In light of increasing needs regarding automated systems availability, safety, and performance, it is necessary to develop a diagnostic module to detect faults that may damage these systems operations and identify their origin or source.

Despite the tangible progress made, researchers must still deal with severe difficulties in controlling such systems, particularly in the presence of faults. Especially in the case of some systems like unmanned aerial vehicles (UAV).

Quadcopters have been the subject of several studies in particular in the field of diagnosis and fault tolerance. (Freddi, Longhi and Monteriù 2010), (Xulin and Yuying 2018), (Ouadine, et al. 2020), (Xiao-Lu 2020)

The work in (Avram, Zhang and Muse 2018) presents a nonlinear robust adaptive fault-tolerant altitude and attitude tracking scheme to accommodate actuator faults in a quadrotor. In (Xulin and Yuying 2018), the authors present a fuzzy active disturbance rejection control method for controlling a quadrotor UAV with actuator faults.

An active fault-tolerant tracking control system approach for actuator faults on a quadrotor was discussed in (Zhong, Liu and Zhang). A fault-tolerant controller was designed on basis of adaptive estimation for actuator faults in (Hasanshahi, Ahmadi and Amjadifard). In (Hong-Jun , Yanli and Tianbo), the authors present the diagnosis and compensation of sensors and actuators faults in a quadrotor UAV based on a nonlinear high-gain observer. Other strategies are proposed in (Yujiang , Youmin and Wei), (Xiao-Lu), (Lien, Chao-Chung and Yi-Hsuan).

In the field of active FTC, observer-based reconstruction and defect estimation (FRE) has gained increased interest in the last two decades. Its advantage is that it can estimate the defects without going through the residual generation phase. Various observer-based FRE design techniques have been presented in the literature, mainly based on sliding-mode observers, observers for singular systems, and adaptive observers (Jiang and Yu 2012). When faults are modeled in terms of parameter changes, adaptive observers can be used to estimate these faults.

This article presents a new fault-tolerant active control technique on a quadrotor in the presence of actuator faults. It is based on a joint use of an adaptive observer for fault reconstruction and estimation and a backstepping approach for system control. Compared to previous work on the active FTC of a quadcopter UAV, in our work we have not neglected the non-linearity of the dynamic model of the quadcopter and the high-order non-holonomic constraints. It was used an adaptive observer proposed in (Oucief, Tadjine, & Labiod, 2016a)

In the first section, the dynamic modeling of the quadcopter is carried out. Then, in the second section, a robust control strategy with actuator faults is established based on the backstepping technique. To detect defects, an adaptive observer was developed to estimate the size of defects. Finally, in the last

section, simulations on MATLAB were carried out to validate the synthesized control laws. The results were conclusive in the presence of faults in the actuators.

1. Quadrotor Modelling

The aerial robot under study consists of a rigid cross frame coupled with four propellers, as illustrated in figure 1. The forward/ backward left/ right and the yaw movements are generated by a differential control strategy of the thrust delivered by each rotor. The up-down motion increases or reduces the overall thrust while keeping an equal individual thrust. To minimize the yaw drift induced by the responsive torques, the quadrotor aircraft is designed so that the set of rotors (right-left) spins clockwise and the set of rotors (front-rear) spins counter-clockwise.

Let E (O, X, Y, Z) designate an inertial frame, and B (o,x,y,z) designate a frame permanently coupled to the quadrotor, as illustrated in figure 1.

The absolute location is denoted by the three coordinates (x, y, z) and its attitude by the three Euler's angles (ϕ, θ, ψ) respectively called Roll angle (ϕ rotation around x-axis), Pitch angle (ϑ rotation around y-axis) and Yaw angle (ψ rotation around z-axis).
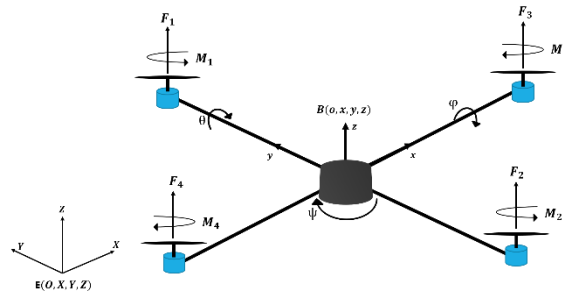

Figure 1. Quadrotor configuration

Literally, by using formalism of Newton-Euler, the quadrotor complete model (position and orientation dynamic) is provided as in (Bouadi, Bouchoucha and Tadjine) by:

$$\ddot{\varphi} = \frac{1}{I_x}\left\{\dot{\theta}\dot{\psi}(I_y - I_x) - K_{fax}\dot{\varphi}^2 - J_r\bar{\Omega}\dot{\theta} + dU_2\right\} \tag{1a}$$

$$\ddot{\theta} = \frac{1}{I_y}\left\{\dot{\varphi}\dot{\psi}(I_z - I_x) - K_{fay}\dot{\theta}^2 - J_r\bar{\Omega}\dot{\varphi} + dU_3\right\} \tag{2b}$$

$$\ddot{\psi} = \frac{1}{I_z}\left\{\dot{\theta}\dot{\varphi}(I_x - I_y) - K_{faz}\dot{\psi}^2 + K_dU_4\right\} \tag{3c}$$

$$\ddot{x} = \frac{1}{m}\left\{(C\varphi S\theta C\psi + S\varphi S\psi)U_1 - K_{ftx}\dot{x}\right\} \tag{4d}$$

$$\ddot{y} = \frac{1}{m}\left\{(C\varphi S\theta S\psi - S\varphi C\psi)U_1 - K_{fty}\dot{y}\right\} \tag{5e}$$

$$\ddot{z} = \frac{1}{m}\left\{(C\varphi C\theta)U_1 - K_{ftz}\dot{z}\right\} - g \tag{6f}$$

Where:
- K_p is the lift coefficient.
- K_d drag coefficient.
- I_x, I_y and I_z constant inertia
- K_{ftx}, K_{fty} and K_{ftz} are the translation drag coefficients.
- K_{fax}, K_{fay} and K_{faz} are the aerodynamic friction coefficients around (X,Y,Z).
- d is the distance between the quadrotor center of mass and the rotation axis of propeller
- J_r is the rotor inertia.

The quadrotor object of our study is (Draganfly IV: Manufactured by Draganfly Innovations). Parameter identification is studied in (Derafa, Madani and Benallegue 2006) (Table)

$K_P = 2.9842 \times 10^{-5}\ N.m/rad/s$ $m = 486\ g$

$(I_x, I_y, I_z) = (3.8278, 3.8278, 7.1345) \times 10^{-3}\ N/_{m.s^2}$ $g = 9.81 m/s^2$

$(K_{fax}, K_{fay}, K_{faz}) = (5.5670, 5.5670, 6.3540) \times 10^{-4} N/rad/s$ $d = 25\ cm$

$(K_{ftx}, K_{fty}, K_{ftz}) = (3.2, 3.2, 4.8) \times 10^{-2} N/m/s$
$J_r = 2.8385 \times 10^{-5}$ N. $m/\text{rad}/s^2$
$K_d = 3.2320 \times 10^{-5}$ N. $m/\text{rad}/s$

U_1, U_2, U_3 and U_4 are the control inputs of the system which are written according to the angular velocities of the four rotors as follows:

$$\begin{bmatrix} U_1 \\ U_2 \\ U_3 \\ U_4 \end{bmatrix} = \begin{bmatrix} K_p & K_p & K_p & K_p \\ -K_p & 0 & K_p & 0 \\ 0 & -K_p & 0 & K_p \\ K_d & -K_d & K_d & -K_d \end{bmatrix} \begin{bmatrix} \omega_1^2 \\ \omega_2^2 \\ \omega_3^2 \\ \omega_4^2 \end{bmatrix} \tag{3}$$

$$\bar{\Omega} = \omega_1 - \omega_2 + \omega_3 - \omega_4 \tag{4}$$

From the equations of the translation dynamics (1) we can deduce the expressions of the high-order nonholonomic constraints:

$$tan\theta = \frac{(\ddot{x} + \frac{K_{ftx}}{m}\dot{x})C\psi + (\ddot{y} + \frac{K_{fty}}{m}\dot{y})S\psi}{\ddot{z} + g + \frac{K_{ftz}}{m}\dot{z}} \tag{5a}$$

$$Sin\,\varphi = \frac{\left(\ddot{x} + \frac{K_{ftx}}{m}\dot{x}\right)S\psi - \left(\ddot{y} + \frac{K_{fty}}{m}\dot{y}\right)C\psi}{\sqrt{\left(\ddot{x} + \frac{K_{ftx}}{m}\dot{x}\right)^2 + \left(\ddot{y} + \frac{K_{fty}}{m}\dot{y}\right)^2 + \left(\ddot{z} + g + \frac{K_{ftz}}{m}\dot{z}\right)^2}} \tag{5b}$$

2. Nonlinear adaptive observer design

2.1. State-space model

The complete model resulting by adding the actuator faults in the model (1a) can be written in the state-space form:

$$\dot{x}(t) = Ax(t) + \Omega(y,u) + B\Phi(x,u) + Ef(x)$$
$$y(t) = Cx(t)\dashv \tag{13}$$

with $x(t) \in \mathbb{R}^n$ is the state vector of the system, such as:

$$x = [x_1, \ldots, x_{12}]^T = \left[\varphi, \theta, \psi, x, y, z, \dot{\varphi}, \dot{\theta}, \dot{\psi}, \dot{x}, \dot{y}, \dot{z}\right]^T \tag{14}$$

and $f(x) = \Psi(x)f_a(t)$, is the resultant vector of actuator faults related to quadrotor motions, with $f_a = [f_{a1}, f_{a2}, f_{a3}, f_{a4}]^T$ represent the actuators faults vector.
$u(t) \in \mathbb{R}^m$ is the input control vector,
$y(t) \in \mathbb{R}^p$ is the output vector, $f_a(t) \in \mathbb{R}^r$ represent the actuators faults vector.
$\Omega(y,u): \mathbb{R}^p \times \mathbb{R}^m \to \mathbb{R}^n$ and $\Phi(x,u): \mathbb{R}^n \times \mathbb{R}^m \to \mathbb{R}^s$ are known nonlinear function vectors and the regressor $\Psi(x): \mathbb{R}^n \to \mathbb{R}^{q \times r}$ is a known function matrix which may depend nonlinearly on x.
$A \in \mathbb{R}^{n \times n}$, $B \in \mathbb{R}^{n \times s}$, $E \in \mathbb{R}^{n \times q}$ and $C \in \mathbb{R}^{p \times n}$ are known constant matrices. Finally, the output vector is giving by $y = [\varphi, \theta, \psi, x, y, z]^T$.
Throughout this paper, the system model (13) has to satisfy the following conditions:
C0: The pair (C, A) must be observable;
C1: The vector function $\eta(y,u)$ is continuous in its variables;
C2: $\Phi(x,u)$ and $\sigma(x)$ satisfy the Lipschitz property with respect to x, i.e., there exist positive constants γ_1 and γ_2 such that:

$$\| \Phi(x,u) - \Phi(\hat{x},u) \| \le \gamma_1 \| x - \hat{x} \| \tag{15a}$$
$$\| \Psi(x) - \Psi(\hat{x}) \| \le \gamma_2 \| x - \hat{x} \| \tag{15b}$$

C3: The fault vector f_a is piecewise constant and bounded in the following sense:
Were

$$\|f_a(t)\| \le \|f_{a_m}\| = \gamma_3 \tag{16}$$

$f_{a_m} \in R^q$ is a known constant vector and γ_3 is a known positive constant.

2.2. The adaptive state observer

The typical form of the adaptive state observer dealing with the class of nonlinear systems (13) is given by the following equations ((Cho and Raramani), (That and Ding)):

$$\dot{\hat{x}}(t) = A\hat{x}(t) + \Omega(y,u) + B\Phi(\hat{x},u) + E\hat{f}(x) + L\,(y - C\hat{x}) \tag{17a}$$

$$\dot{\hat{f}}(t) = \rho^{-1}\Psi(\hat{x})^T FC(x - \hat{x}) \tag{17b}$$

where $\hat{x}$ is the state estimate, $\hat{f}(x) = \Psi(x)\hat{f}_a(t)$. $\hat{f}_a(t)$ is the unknown parameter vector estimate. $L \in \mathbb{R}^{n\times p}$ is the observer gain, ρ is a positive constant and $F \in \mathbb{R}^{q\times p}$ is a matrix to be designed.

Under conditions 1, 2 and 3, the state estimate $\hat{x}$ converges to the actual state x and $E\hat{f}(x)$ converges to $Ef(x)$, if there exist a symmetric positive definite matrix $P \in \mathbb{R}^{n\times n}$ and a matrix $F \in \mathbb{R}^{q\times p}$ such that (Cho and Raramani):

$$E^T P = FC \tag{18}$$

Equality (18) is known as the observer matching condition (Floquet, Edwards and Spurgeon), it hold if and only if ((Corless and Tu); (Raoufi , Jose Marquez and Solo)):

$$rank(CE) = rank(E) \tag{19}$$

It is easy to check that the observer matching condition (18) is not satisfied for our system and hence no adaptive observer of the form presented in (Cho and Raramani) and (That and Ding) can be used to estimate x and θ.

In (Oucief, Tadjine and Labiod , A new methodology for an adaptive state observer design for a class of nonlinear systems with unknown parameters in unmeasured state dynamics), authors have developed an adaptive observer for a certain class of non-linear systems. This observer employs the nonlinear system model described by equation (13).

For developing the considered adaptive observer, in addition to conditions C0, C1, C2 and C3 the system model (13) has to satisfy the following conditions:

C4: The matrices A, B, E and C satisfy the following conditions:

$$CB = 0_{p\times s} \tag{20a}$$

$$CE = 0_{p\times r} \tag{20b}$$

$$rank(CAE) = rank(E) \tag{20c}$$

C5: The first derivative in time of $\Psi(x)$ is continuous and bounded provided that x is bounded.

To satisfies the condition C4 giving by equation (20), the state space is rearranged. From equations (1) and considering the actuator faults, we obtain:

$$\dot{x}_1 = x_7 \tag{21a}$$

$$\dot{x}_2 = x_8 \tag{21b}$$

$$\dot{x}_3 = x_9 \tag{21c}$$

$$\dot{x}_4 = x_{10} \tag{21d}$$

$$\dot{x}_5 = x_{11} \tag{21e}$$

$$\dot{x}_6 = x_{12} \tag{21f}$$

$$\dot{x}_7 = a_1 x_8 x_9 + a_2 x_7^2 + a_3 \bar{\Omega} x_8 + b_1(U_2 + f_{a1}) \tag{21g}$$

$$\dot{x}_8 = a_4 x_7 x_9 + a_5 x_8^2 + a_6 \bar{\Omega} x_7 + b_2(U_3 + f_{a2}) \tag{21h}$$

$$\dot{x}_9 = a_7 x_7 x_8 + a_8 x_9^2 + b_3(U_4 + f_{a3}) \tag{21i}$$

$$\dot{x}_{10} = a_9 x_{10} + U_x \frac{U_1}{m} \tag{21j}$$

$$\dot{x}_{11} = a_{10} x_{11} + U_y \frac{U_1}{m} \tag{21k}$$

$$\dot{x}_{12} = a_{11} x_{12} - g + \frac{cos(x_1)\,cos(x_2)}{m}(U_1 + f_{a4}) \tag{21l}$$

With

$$a_1 = \frac{I_y - I_z}{I_x} \qquad a_2 = \frac{-K_{fax}}{I_x} \qquad a_3 = \frac{-J_r}{I_x} \qquad a_4 = \frac{I_z - I_x}{I_y} \qquad a_5 = \frac{-K_{fay}}{I_y} \tag{22}$$

$$a_6 = \frac{J_r}{I_y} \qquad a_7 = \frac{I_x - I_y}{I_z} \qquad a_8 = \frac{-K_{faz}}{I_z} \qquad a_9 = \frac{-K_{fax}}{m} \qquad a_{10} = \frac{-K_{fay}}{m}$$

$$a_{11} = \frac{-K_{faz}}{m} \qquad b_1 = \frac{d}{I_x} \qquad b_2 = \frac{d}{I_y} \qquad b_3 = \frac{1}{I_z}$$

When these conditions are satisfied, a stable observer for the system (13) has the form (Oucief, Tadjine and Labiod , A new methodology for an adaptive state observer design for a class of nonlinear systems with unknown parameters in unmeasured state dynamics):

$$\dot{\hat{x}}(t) = A\hat{x}(t) + \Omega(y,u) + B\Phi(\hat{x},u) + E\hat{f}(x) + L\,(y - C\hat{x}) \tag{24a}$$

$$\hat{f}_a(t) = W + \Gamma\Psi^T(\hat{x})Hy \tag{24b}$$

$$\dot{W} = -\Gamma\frac{d\Psi^T(\hat{x})}{dt}Hy - \Gamma\Psi^T(\hat{x})[HC(A\hat{x}(t) + \Omega(y,u)) + G\,(y(t) - C\hat{x}(t))] \tag{24c}$$

$\hat{f}(x) = \Psi(\hat{x})\hat{f}_a(t)$. ($\hat{f}_a(t)$ is the unknown parameter vector).

H and G are constant matrices to be designed and $\Gamma = \Gamma^T > 0$ is the learning rate matrix.

A sufficient condition for the asymptotic stability of the adaptive state observer is described in the following theorem.

Theorem 2. (Oucief, Tadjine and Labiod , A new methodology for an adaptive state observer design for a class of nonlinear systems with unknown parameters in unmeasured state dynamics)

Under conditions 0, 1, 2, 3, 4 and 5, the estimate of the state $\hat{x}$ converges to the real state x asymptotically while $E\hat{f}(x)$ converges to $Ef(x)$ if there are positive real constants ε_1 and ε_2 and matrices $P = P^T > 0$, H and G such that :

$$(A - LC)^T P + P(A - LC) + \varepsilon_1 PBB^T P + \varepsilon_2 PEE^T P + \varepsilon_1^{-1}\gamma_1 I_n + \varepsilon_2^{-1}\gamma_2^2\rho I_n < 0 \tag{25a}$$

$$HCA - GC = E^T P \tag{25b}$$

However, condition C4 is satisfied, and as a consequence, the adaptation law (24) is feasible. Notice that according to the structure of the matrices C and E, the system is already in the form (13) and therefore no state transformation is needed to design the adaptive observer.

As the state, input, fault and output vector, respectively, then the system described in (21) can be rewritten as a state space system of the form (13), where

$$\Omega(y,u) \quad = 0_{(12\times1)} \tag{23a}$$

$$\Phi(x,u) \quad = [a_1 x_4 x_6 \quad a_2 x_2^2 \quad a_3\bar{\Omega}x_4 \quad b_1 U_2 \quad a_4 x_2 x_6 \quad a_5 x_4^2 \quad a_6\bar{\Omega}x_2 \quad b_2 U_3 \quad a_7 x_2 x_4$$

$$a_8 x_6^2 \quad b_3 U_4 \quad U_x\frac{U_1}{m} \quad U_y\frac{U_1}{m} \quad \frac{\cos(x_1)\cos(x_2)}{m}U_1 - g]^T \tag{23b}$$

$$\Psi(x) \quad = diag\left(b_1, b_2, b_3, \frac{\cos(x_1)\cos(x_2)}{m}\right) \tag{23c}$$

2.3. Observer design

The objective of this part is to synthesize an adaptive state observer corresponding to the model quadrotor given by (23) which can be described in the form of system given by (13).

Since $\Psi(x)$ is a matrix, the computation of its Lipschitz constant γ_2 is not a trivial task. In order to do this, we evaluate the Lipschitz constants of the individual rows of $\sigma(x)$.

$$\|\sigma(x) - \sigma(\hat{x})\| \leq max\left(\left\|\frac{\partial\Psi(sat(x))}{\partial x}\right\|\right)\|x - \hat{x}\| \tag{26c}$$

The computation of γ_2 is given by

$$max\left(\left\|\frac{\partial\Psi(sat(x))}{\partial x}\right\|\right) = max\left(\left\|-\frac{1}{m}[sin(x_1)cos(x_2) + cos(x_1)sin(x_2)]\right\|\right)$$

$$= max\left(\left\|-\frac{1}{m}sin(x_1 + x_2)\right\|\right) \tag{27}$$

We found that we can take $\gamma_2 = 2.058$.

The function $\Phi(x,u)$ is given by:

$$\Phi(x,u) = [a_1 x_4 x_6 \quad a_2 x_2^2 \quad a_3\bar{\Omega}x_4 \quad b_1 U_2 \quad a_4 x_2 x_6 \quad a_5 x_4^2 \quad a_6\bar{\Omega}x_2 \quad b_2 U_3 \quad a_7 x_2 x_4 \tag{28}$$

$$\left. \begin{matrix} a_8 x_6^2 & b_3 U_4 & U_x \dfrac{U_1}{m} & U_y \dfrac{U_1}{m} & \dfrac{cos(x_1)\,cos(x_2)}{m} U_1 - g \end{matrix} \right]^T$$

However, $\Phi(x,u)$ is locally Lipschitz, which means that its Lipschitz constant γ_1 depends on the region where the system operates. Suppose that the control input is chosen such that it keeps the state bounded in the set

$$\Omega_1 = \left\{ (x_1, x_2, x_3, x_4, x_5, x_6) \in \mathbb{R}^6 / |x_1| < \frac{\pi}{2}, |x_2| < \frac{\pi}{2}, |x_3| < \pi, |x_4| < 5, |x_5| < 10, |x_6| < 20 \right\} \quad (29)$$

Then $\Phi(x,u)$ can be extended into the bounded function $\Phi(sat(x))$ which coincides with $\Phi(x,u)$ in Ω_1, and thus the system becomes globally Lipschitz (Farza, M'Saad and Maatoug), γ_1 can be computed using the relation $\gamma_1 = max(\left\| \frac{\partial \Phi(sat(x))}{\partial x} \right\|)$. The computation of γ_1 is given by

$$\gamma_1 = max\left(\left\| \frac{\partial \Phi(sat(x))}{\partial x} \right\| \right) = 34.82 \quad (30)$$

Where $X = 5$, $Y = 10$, $z = 20$. Which yields $\gamma_1 = 34.82$.
Since $f_a(t)$ is a matrix, the computation of γ_3 is given by

$$\gamma_3 = max(\|f_a(t)\|) = 10.18 \quad (31)$$

Where $f_{a_{mi}}$ are the known constant vector. Finally, the bound in conditions C3 can be chosen as $\gamma_3 = 10.18$.

We start the observer design by computing the observer gains presented in (24). Let $\varepsilon_1 = 76$ and $\varepsilon_2 = 80$. Finding the observer gains by solving (25a) under equality constraint (25b) is not a trivial task. To make this problem easily tractable, we intend in this subsection to transform it into an LMI optimization problem. By introducing the following change of variable

$$L = P^{-1}M \quad (32)$$

where $M \in \mathbb{R}^{n \times p}$ and using the Schur complement (Boyd, El Ghaoui and Feron), inequality (25a) can be turned into the following LMI in the variable P

$$\begin{bmatrix} \Lambda & PB & PE \\ B^T P & -\varepsilon_1^{-1} I_s & 0_{s \times q} \\ E^T P & 0_{q \times s} & -\varepsilon_2^{-1} I_q \end{bmatrix} < 0 \quad (33)$$

where $\Lambda = A^T P + PA - C^T M^T - MC + \varepsilon_1^{-1} \gamma_1^2 I_n + \varepsilon_2^{-1} \gamma_2^2 \gamma_3^2 I_n$.
Also, by using the same idea used in (Corless and Tu) we can turn the problem of the resolution of equality (15b) into the following LMI optimization problem.
Minimize δ subject to

$$\begin{bmatrix} \delta I_q & \Pi \\ \Pi^T & \delta I_n \end{bmatrix} \geq 0 \quad (34)$$

Where $\Pi = HCA - GC - E^T P$, and δ is a positive scalar. Therefore, computing P,H, and G involves solving LMIs (21) and (22), simultaneously, for $P = P^T > 0$, $M = M^T$.
The LMIs were solved using CVX, a Matlab-based modelling system for convex optimization (Grant , Boyd and Ye). we obtain the following results

$$M = [M_1 \; M_2]^T \quad (35)$$

Where

$$M_1 = diag(1.567,1.567,1.312,0.429,0.429,0.731)$$
$$M_2 = diag(0.815,0.815,0.779,0.455,0.455,0.475)$$
$$H = diag(0.0118,0.0118,0.0151,0.0311),$$
$$G = diag(2.738,2.738,2.761,0.000,2.873)$$
$$\delta = 1.0001 \times 10^{-5} \quad (36)$$
$$L = [L_1 \; L_2]^T \quad (37)$$
$$L_1 = diag(980,980,500,60,60,200)$$
$$L_2 = 10^5 \times diag(2.96,2.96,1.41,0.09,0.09,0.34)$$

The unknown parameter vector estimates $\hat{f}_a(t)$ and confirming to (24) is then

$$\dot{\hat{f}}_a(t) = \Gamma \sigma^T(\hat{x}) E^T P e_x \quad (38)$$

$$\hat{\dot{f}}_a(t) = \begin{bmatrix} \hat{\dot{f}}_{a1} \\ \hat{\dot{f}}_{a2} \\ \hat{\dot{f}}_{a3} \\ \hat{\dot{f}}_{a4} \end{bmatrix} = 10^3 \begin{bmatrix} 7.475e_7 - 1743.4e_1 \\ 7.436e_8 - 1733.9e_2 \\ 19.130e_9 - 3497.9e_3 \\ (0.302e_{12} - 57.34e_6)\,c\,x_1\,c\,x_2 \end{bmatrix} \tag{39}$$

Where $e_i = x - \hat{x}$ and $e_i = x_i - \hat{x}_i$ are the tracking-errors of x and x_i respectively. $c\,x_1 = cos(x_1)$ and $c\,x_2 = cos(x_2)$.

3. Control Strategy of Quadrotor with Actuator Faults

3.1. Control Strategy

Generally, a fault-tolerant system is composed of two cascaded modules. The first one is a monitoring module which is used to detect faults, and diagnose their location and significance in a system. The second is a recovery module taking necessary actions so that the faulty system can achieve the control objectives almost at any time (Jain, J. Yamé and Sauter).

In our case, an adaptive observer is used like a monitoring module (Figure 2) and the recovery module is based on the Backstepping approach.
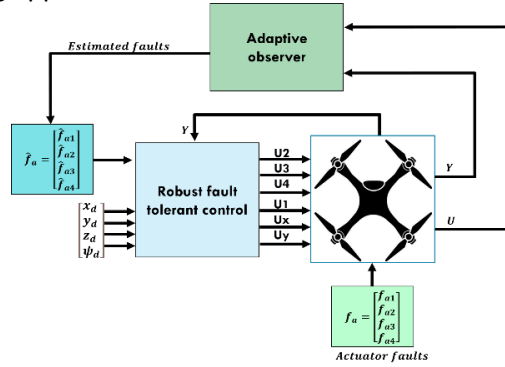

Figure 2. Fault-tolerant control system architecture

The following assumptions are needed for the analysis:

Assumption 1: (justifier physiquement toutes ces hypothèses)
The resultant of actuator faults related to quadrotor motions are slowly varying in time and bounded, as follows:

$$\begin{cases} \dot{f}(t)_{ai} \approx 0 \\ |f_{ai}(t)| \leq f_{ai}^+ \end{cases} \qquad i \in [1,2,3,4] \tag{40}$$

Where $\{f_{a1}^+, f_{a2}^+, f_{a3}^+, f_{a4}^+\}$ are positive constants.

Assumption 2:
The unknown's parts $f(x, f_{ai}, t)$ including the resultants of actuator faults related to the quadrotor motions are also bounded:

$$|f(x, f_{ai}, t)| \leq |\sigma_i(x,t)| f_{ai}^+ \leq k_{ai} \tag{41}$$

Where $\{k_{a1}, k_{a2}, k_{a3}, k_{a4}\}$ are positive constants.

The proposed control approach is based on two loops (internal loop and external loop). The internal loop has four control laws: control of roll, control of pitch, control of yaw, and control of altitude. The external loop has two control laws of coordinates x and y.

The external control loop produces the desired roll (φ_d) and pitch (θ_d) via the corrective block (shown by equation (5)). The corrective block has as a goal to correct the rotation of the roll and pitch based on the desired yaw (ψ_d). The synoptic scheme (Figure 3) below illustrates this control strategy:
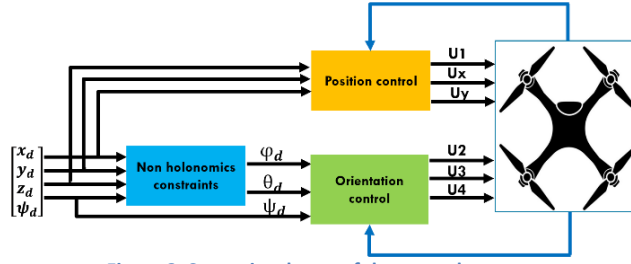
Figure 3. Synoptic scheme of the control strategy

3.2. Control laws

Based on the backstepping technique, an iterative algorithm is used to synthesize the control laws forcing the system to follow the desired path in presence of actuator failures, we summarize all stages of calculation concerning the tracking errors and Lyapunov functions in the following way:

$$e_i = \begin{cases} x_{id} - x_i & i \in [1,2,3,4,5,6] \\ \dot{x}_{(i-1)d} + k_{(i-1)}e_{(i-1)} - x_i & i \in [7,8,9,10,11,12] \end{cases} \tag{42}$$

$$c_i > 0 \quad i \in [1,\dots,12]$$

The related Lyapunov functions are provided by:

$$V_i = \begin{cases} \dfrac{1}{2}e_i^2 & i \in [1,2,3,4,5,6] \\ V_{i-1} + \dfrac{1}{2}e_i^2 + e_x^T P e_x + e_f^T \Gamma^{-1} e_f & i \in [7,8,9,10,11,12] \end{cases} \tag{43}$$

The synthesized stabilizing control laws are as described in the following:

$$U_2 = \frac{1}{b_1}\left[\ddot{\varphi}_d + e_1 + k_2 e_2 + k_1(-k_1 e_1 + e_2) - a_1 x_8 x_9 - a_2 x_7^2 - a_3 \bar{\Omega} x_8 - \hat{f}_1(x)\right] \tag{44a}$$

$$U_3 = \frac{1}{b_2}\left[\ddot{\theta}_d + e_3 + +k_4 e_4 + k_3(-k_3 e_3 + e_4) - a_4 x_7 x_9 - a_5 x_8^2 - a_6 \bar{\Omega} x_7 - \hat{f}_2(x)\right] \tag{44b}$$

$$U_4 = \frac{1}{b_3}\left[\ddot{\psi}_d + e_5 + k_6 e_6 + k_5(-k_5 e_5 + e_6) - a_7 x_7 x_8 - a_8 x_9^2 - \hat{f}_3(x)\right] \tag{44c}$$

$$U_x = \frac{m}{U_1}\left[\ddot{x}_d + e_7 + k_8 e_8 + k_7(-k_7 e_7 + e_8) - a_9 x_{10}\right] \tag{44d}$$

$$U_y = \frac{m}{U_1}\left[\ddot{y}_d + e_9 + k_{10} e_{10} + k_9(-k_9 e_9 + e_{10}) - a_{10} x_{11}\right] \tag{44e}$$

$$U_1 = \frac{m}{\cos(x_1)\cos(x_2)}\left[\ddot{z}_d + e_{11} - k_{12} e_{12} + k_{11}(-k_{11} e_{11} + e_{12}) - a_{11} x_{12} + g - \hat{f}_4(x)\right] \tag{44f}$$

Proof

Considering the first subsystem:

$$\begin{cases} \dot{x}_1 = x_7 \\ \dot{x}_7 = a_1 x_8 x_9 + a_2 x_7^2 + a_3 \bar{\Omega} x_8 + b_1(U_2 + f_{a1}) \end{cases} \tag{45}$$

The corresponding reduced order observer is:

$$\begin{cases} \dot{\hat{x}}_1 = \hat{x}_7 + l_1(y_1 - \hat{y}_1) \\ \dot{\hat{x}}_7 = a_1 \hat{x}_8 \hat{x}_9 + a_2 \hat{x}_7^2 + a_3 \bar{\Omega} \hat{x}_8 + b_1(U_2 + \hat{f}_{a1}) + l_2(y_2 - \hat{y}_2) \end{cases} \tag{46}$$

The calculation of the command U_2 is done in two steps.

Step 1: For the first step we consider the first tracking-error e_1 given by

$$e_1 = x_{1d} - x_1 \tag{46}$$

Let the first Lyapunov function candidate:

$$V_1 = \frac{1}{2}e_1^2 \tag{47}$$

The time derivative of (47) is given by:

8

$$\dot{V}_1 = e_1\dot{e}_1 = e_1(\dot{x}_{1d} - \dot{x}_1) = e_1(\dot{x}_{1d} - x_7) \tag{48}$$

The stabilization of e_1 can be obtained by introducing a new virtual control x_7:

$$(x_7)_d = \alpha_1 = \dot{x}_{1d} + k_1 e_1 \quad (k_1 > 0) \tag{49}$$

The equation (48) is then

$$\dot{V}_1 = -k_1 e_1{}^2 \leq 0 \tag{50}$$

Step 2: For the second step we consider the following tracking-error e_2 given by

$$e_2 = \alpha_1 - x_7 = \dot{x}_{1d} + k_1 e_1 - x_7 \tag{51}$$

Let $e_x = x - \hat{x}$ and $e_f = f_a - \hat{f}_a$ and from (40) notice that $\dot{f}(t)_{ai} \approx 0$.
Then, from (13) and (24), it follows that

$$\dot{e}_x = (A - LC)e_x + B\tilde{\Phi} + E(\tilde{\sigma}\theta + \sigma(\hat{x})e_f) \tag{52}$$

$$\dot{e}_f = -\Gamma\sigma^T(\hat{x})(HCA - GC)e_x \tag{53}$$

Where $\tilde{\sigma} = \sigma(x,u) - \sigma(\hat{x},u)$ and $\tilde{\Phi} = \Phi(x,u) - \Phi(\hat{x},u)$.
The augmented Lyapunov function is given by:

$$V_2 = V_1 + \frac{1}{2}e_2^2 + e_x^T P e_x + e_f^T \Gamma^{-1} e_f = V_1 + \frac{1}{2}e_2^2 + V_T \tag{54}$$

The time derivative of V_2 is given by:

$$\dot{V}_2 = \dot{V}_1 + e_2\dot{e}_2 + \dot{V}_T \tag{55}$$

The time derivative of $V_T = e_x^T P e_x + e_f^T \Gamma^{-1} e_f$ is given by:

$$\dot{V}_T = 2e_x^T P \dot{e}_x + 2e_f^T \Gamma^{-1} \dot{e}_f \tag{56}$$

Substituting (52) and (53) into (56) yields

$$\dot{V}_T = 2e_x^T P(A - LC)e_x + 2e_x^T PB\tilde{\Phi} + 2e_x^T PE\tilde{\sigma}\theta + 2e_x^T PE\sigma(\hat{x})e_f - 2e_f^T \sigma^T(\hat{x})(HCA - GC)e_x \tag{57}$$

Using (25b), we get:

$$\dot{V}_T = e_x^T[(A - LC)^T P + P(A - LC)]e_x + 2e_x^T PB\tilde{\Phi} + 2e_x^T PE\tilde{\sigma}\theta \tag{58}$$

By using $2u^T v \leq \varepsilon u^T u + \varepsilon^{-1}v^T v$ the Lipschitz conditions (15a) to (15b), and inequality (16), we obtain the following inequalities

$$2e_x^T PB\tilde{\Phi} \leq \varepsilon_1 e^T{}_x PBBP e_x + \varepsilon_1{}^{-1}\tilde{\Phi}^T \tilde{\Phi}$$
$$\leq \varepsilon_1 e_x PBBP e_x + \varepsilon_1{}^{-1}e^T{}_x \gamma_1{}^2 e_x \tag{59}$$

and

$$2e_x^T PE\tilde{\sigma}\theta \leq \varepsilon_2 e^T{}_x PEEP e_x + \varepsilon_2{}^{-1}\theta^T \tilde{\sigma}^T \tilde{\sigma}\theta$$
$$\leq \varepsilon_2 e^T{}_x PEEP e_x + \varepsilon_2{}^{-1}e_x{}^T \gamma_2{}^2 \gamma_3{}^2 e_x \tag{60}$$

where ε_1 and ε_2 are positive constants. Substituting (59) and (60) into (58), we obtain

$$\dot{V}_T \leq -e_x{}^T Q e_x \tag{61}$$

Substituting (61) into (55) yields

$$\begin{aligned}
\dot{V}_2 &\le -k_1 e_1{}^2 + e_2[e_1 + \dot{e}_2] - e_x{}^T Q e_x \\
&\le -k_1 e_1{}^2 - k_2 e_2{}^2 + e_2[k_2 e_2 + e_1 + \ddot{\varphi}_d + k_1(-k_1 e_1 + e_2) - a_1 x_8 x_9 - \\
&\quad a_2 x_7^2 - a_3 \bar{\Omega} x_8 - b_1 U_2 - b_1 f_{a1}] - e_x{}^T Q e_x \\
&\le -k_1 e_1{}^2 - k_2 e_2{}^2 + e_2[k_2 e_2 + e_1 + \ddot{\varphi}_d + k_1(-k_1 e_1 + e_2) - a_1 x_8 x_9 \\
&\quad -a_2 x_7^2 - a_3 \bar{\Omega} x_8 - b_1 U_2 - b_1 f_{a1}] - c_1 \|e_x\|^2
\end{aligned} \tag{62}$$

Where $\quad \lambda_{min}(Q)$.

By replacing f_{a1} by the estimate $\hat{f}_{a1}$ the stabilization of (e_1, e_2) can be obtained by introducing the input control U_2:

$$U_2 = \frac{1}{b_1}\left[\ddot{\varphi}_d + e_1 + k_2 e_2 + k_1(-k_1 e_1 + e_2) - a_1 x_8 x_9 - a_2 x_7^2 - a_3 \bar{\Omega} x_8 - \hat{f}_1(x)\right] \tag{63}$$

The same steps are followed to extract U_3, U_4, U_x, U_y and U_1.

4. Simulation Results

To evaluate the performance of the controller proposed in this work, we executed test simulations in MATLAB. In the first test (Test 1), the motion of the quadrotor is considered normal without faults. In the second test (Test 2), we created multiple actuator failures $\{f_{a1}, f_{a2}, f_{a3}, f_{a4}\}$ relating to roll, pitch, yaw, and altitude motions.

Results without faults (Test 1) are shown in Figure 4, Figure 7, Figure 9 and Figure 11. The state estimates are shown in Figure 4.
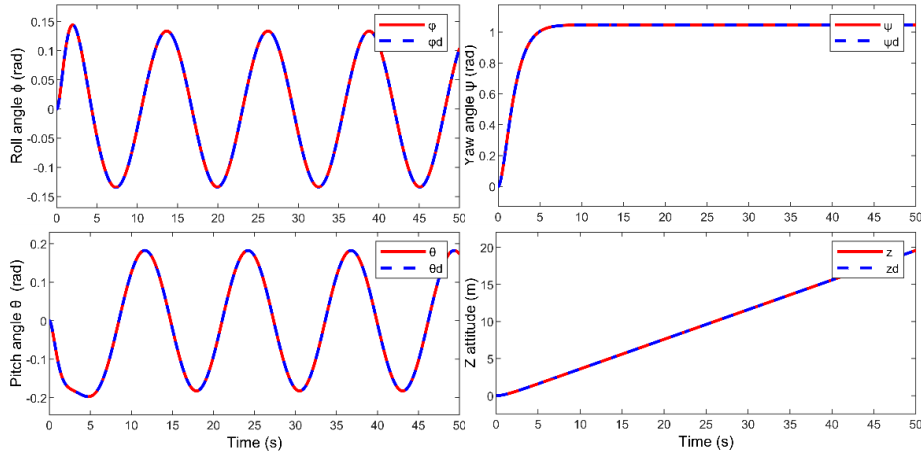

Figure 4. Tracking simulation results of trajectories along roll (φ), pitch (θ), yaw angle (ψ), and Attitude Z axis (Test 1)

From these simulation results (Figure 4), it can be seen that the true and estimated state by using this adaptive observer are matched perfectly. As displayed in Figure 4, the estimation errors respectively of φ, θ, ψ and z are 10^{-5}, 10^{-6}, 10^{-10} and 10^{-5}, which clearly illustrates good performances and robustness towards stability and tracking of this control strategy with respect to the backstepping approach in the absence of faults.

In these tests (Test 2), four actuator faults $\{f_{a1}, f_{a2}, f_{a3}, f_{a4}\}$ related to roll, pitch, yaw and altitude motions (φ, θ, ψ, z) is simulated with 150% of maximum values of inputs control U_2, U_3, U_4 and 100% maximum value of input control U_1 between the instants 10s and 20s and start decreasing between 20s and 40s.

The results of these tests are shown in Figure 5, Figure 8, Figure 10 and Figure 12. The fault's evolution and their estimates are given in Figure 5.
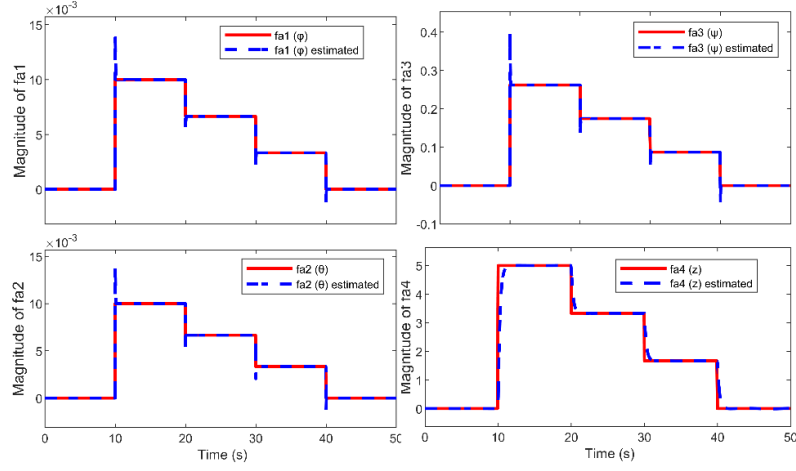
Figure 5. Fault estimation (Test 2)

According to Figure 5, there is very excellent estimation of the actuator faults, even the presence of transient peaks in the discontinuous points (10s, 20s, 30s and 40s). After fault injection in the motors, the estimate of f_{a1}, f_{a2} and f_{a3} converges rapidly to the real values. Meanwhile, the estimate of f_{a4} converge rapidly after 0,4 s. As displayed in Figure 5, the estimation errors respectively of f_{a1}, f_{a2}, f_{a3} and f_{a4} are $10^{-7}, 10^{-6}, 10^{-2}$ and 10^{-2}.Therefore, the proposed observer can give a fast and accurate fault estimation.
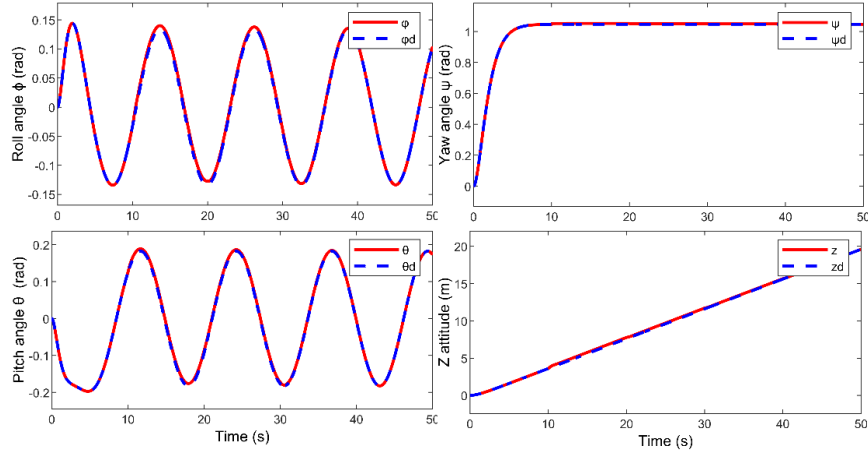

Figure 6. Tracking simulation results of trajectories along roll (ϕ), pitch (θ), yaw angle (ψ), and Attitude Z axis (Test 2)

As displayed in Figure 6, there is very excellent tracking of the intended trajectories even after the appearance of actuator faults. Moreover, we can observe well the tracking of the planned trajectories, with small transient variations in roll, pitch, yaw, and altitude movements in the instants of occurrence of faults (10s, 20s, 30s and 40s).

Therefore, the estimation errors of roll (ϕ), pitch (θ) and yaw (ψ) still keep close to zero ($\approx 10^{-3}$), meanwhile, the estimation error of attitude Z still remain below after 0,2 m. Despite that, the trajectory tracking of our system is assured.

This figure illustrates the advantage of this method over FDI techniques is that the used observer for FRE can also be used for state feedback control because it is designed to preserve accurate state estimation even in the faulty case.
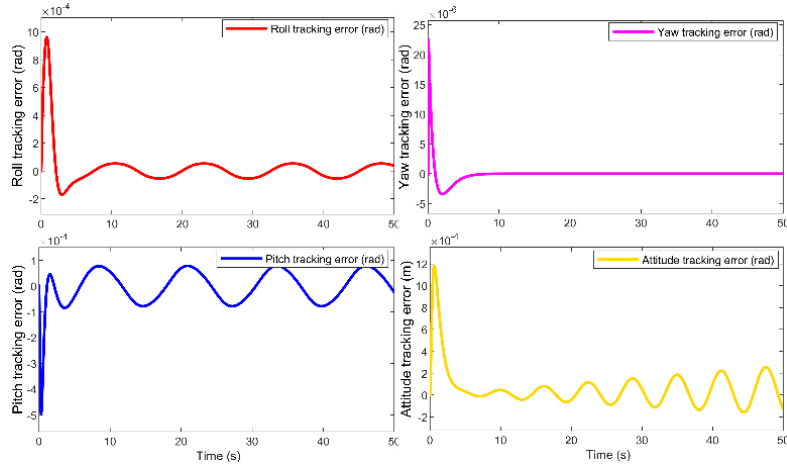
11

Figure 7. Error tracking results of trajectories along roll (ϕ), pitch (θ), yaw angle (ψ), and Attitude Z axis (Test 1)

Figure 7 illustrate the error tracking results of trajectories along roll (ϕ), pitch (θ), yaw (ψ), and attitude Z in absence of actuator faults (Test 1). We can see that the errors converge rapidly to 0 and remain below 10^{-4}.

While, as displayed in Figure 8, the estimation errors of roll (ϕ), pitch (θ) and yaw (ψ) still keep close to zero ($\approx 10^{-3}$), meanwhile, the estimation error of attitude Z still remain below after 0,2 m which represent 4% of the desired attitude.

Figure 9 and Figure 10 illustrate the inputs control $\{U_1, U_2, U_3, U_4\}$ of our system. It is easy to notice the transient peaks in all controllers.

Despite it, the stability of the closed-loop dynamics of the quadrotor is assured. Furthermore, we can observe input control signals provided by this control strategy (Test 1 and Test 2) are acceptable and physically realizable.
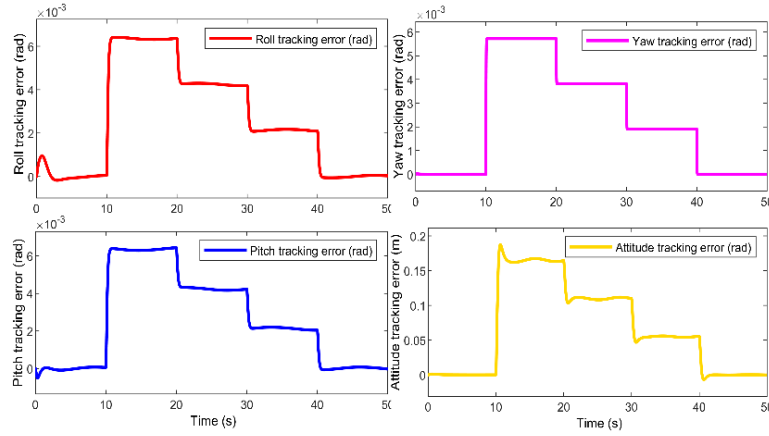

Figure 8. Error tracking results of trajectories along roll (ϕ), pitch (θ), yaw angle (ψ), and Attitude Z axis (Test 2)
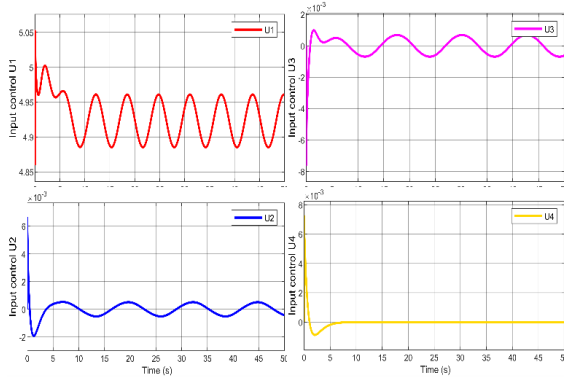

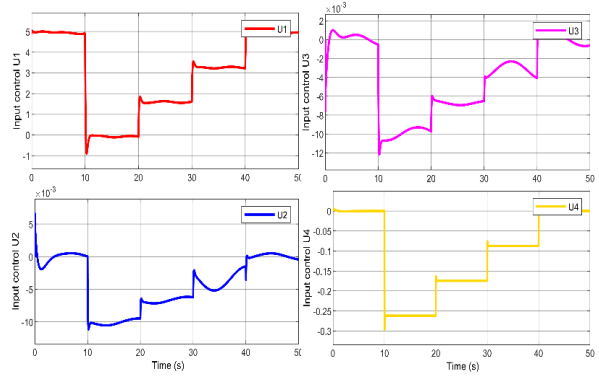**Figure 9. Control inputs of actuators in normal case (Test 1)**

Figure 10. Control inputs of actuators in faulty case (Test 2)

To judge the results obtained in the two tests numerically, we will compute two numerical criteria: the RMS (Root Mean Square) error and the error mean. The results obtained are presented in the table below (Table 1).

	RMS				Error mean			
	ϕ	θ	ψ	Z	ϕ	θ	ψ	Z
Test 1	$1,4.10^{-4}$	7.10^{-5}	$1,8.10^{-6}$	$1,9.10^{-4}$	$1,9.10^{-5}$	$3,2.10^{-6}$	$2,9.10^{-10}$	$6,3.10^{-5}$
Test 2	$3,5.10^{-3}$	$3,5.10^{-3}$	$3,2.10^{-3}$	$9,2.10^{-2}$	$2,2.10^{-3}$	$3,5.10^{-3}$	$2,3.10^{-3}$	$6,6.10^{-2}$

We note that the RMS for the orientation coordinates (ϕ, θ, ψ) is of the order of 10^{-3} and of the order of 10^{-2} for the Z altitude coordinate in faulty case (Test 2) and the same remark for the error mean in faulty case. The quantitative analysis confirms that the proposed strategy not only ensures a satisfactory tracking performance of the state estimation but also preserves a low energy consumption with small control inputs.

Figure 11 and Figure 12 illustrate the 3D trajectory of the quadrotor aircraft throughout the flight. The simulation results shown by this figure indicate high performances and resilience towards stability and tracking even after the occurrence of actuator faults (Figure 12), which shows the efficacy of the control method suggested in this work.
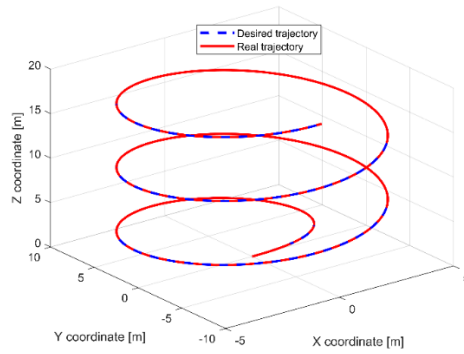

Figure 11. Global trajectory of the quadrotor in 3D along the (X, Y, Z) axis (Test 1)
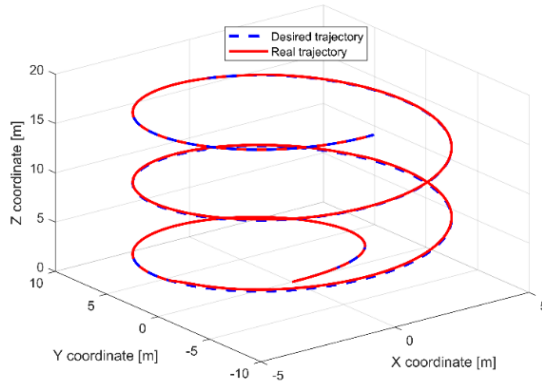

Figure 12. Global trajectory of the quadrotor in 3D along the (X, Y, Z) axis (Test 2)

5. Conclusion

This paper presents a novel active fault-tolerant control strategy for diagnosing the actuator faults for a quadrotor vehicle. This approach is based on the observer-based fault reconstruction and estimation (FRE) technique using an adaptive observer. Firstly, we introduced a complete nonlinear dynamical model of the quadrotor, taking into consideration several physics phenomena that might impact our system's navigation in space. Secondly, we presented a stabilizing control law, in the presence of actuator faults, based on backstepping technique. Thirdly, an adaptive observer has been developed to estimate simultaneously the system state used in feedback control and actuator faults used in the FDI task.

Many test simulations in MATLAB have been executed to evaluate the performance of the proposed strategy. In the first test, the motion of the quadrotor is considered normal without faults. In the second test, we created multiple actuator failures relating to roll, pitch, yaw, and altitude motions. Simulation results clearly illustrates good performances and robustness towards stability and tracking

of this control strategy with respect to the backstepping approach in the absence of faults. There is very excellent estimation of the actuator faults and the intended trajectories even after the appearance of actuator faults. We can see that the errors converge rapidly to 0 and remain below 10^{-4}. While the estimation errors of roll (ф), pitch (θ) and yaw (ψ) still keep close to zero ($\approx 10^{-3}$), meanwhile, the estimation error of attitude Z still remain below 0,2 *m* which represent 4% of the desired attitude. Furthermore, we can observe input control signals provided by this control strategy are acceptable and physically realizable.

The contribution of this work, firstly, is the use of a complete model of the quadrotor considering the non-linearities and the high-order nonholonomic constraints of the system which gives a real behavior of the quadrotor, especially in faulty cases. Secondly, It's the first use of the adaptive observer proposed in (Oucief, Tadjine, & Labiod , 2016a), in the field of active FTC for quadrotor UAV. This observer can estimate the system state and actuator faults simultaneously, which can be used respectively in feedback control and the FDI task of the actuator faults. Another advantage of the use of this observer structure lies in the fact that neither the conventional adaptive state observer nor any other alternative to the adaptive observer can be used in FTC in the case of our complete nonlinear dynamical model of the quadrotor UAV because of the non-satisfaction of the persistent excitation condition by model used. While using an adaptive observer as proposed in (Oucief, Tadjine, & Labiod , 2016a) does not require the system structure to satisfy the standard observer matching condition required in the conventional adaptive state observer. Finally, the use of these observers allows the estimation of any number of faults, regardless of the number of measured outputs, and it can estimate additive and multiplicative faults. The observer gains can be solved together with the Lyapunov inequality using LMI-based computations and do not require to change the system model into a special form like in (Oucief, Tadjine, & Labiod, 2016b) or the resolution of a system of partial differential equations like in (Stamnes, Aamo, & Kaasa, 2011).

This strategy can be easily applied to other nonlinear systems faults tolerant where several faults occur simultaneously. or the process itself in the case where sensor faults occur.

The simulation results have demonstrated the excellent effectiveness of this control strategy, and it maintains the stability and performance of the quadrotor even in the occurrence of actuator faults.

The observer can estimate the system state and actuator faults simultaneously. Neither the conventional adaptive state observer nor any other alternative to the adaptive observer can be used in FTC in the case of our complete nonlinear dynamical model of the quadrotor UAV because of the non-satisfaction of the persistent excitation condition (for more details see section 2.2).(reformule et expliquer d'avantage pourquoi ce n'est pas possible avec les autres méthodes?)

While using an adaptive observer as proposed in (Oucief, Tadjine, & Labiod , 2016a) does not require the system structure to satisfy the standard observer matching condition required in the conventional adaptive state observer. Thirdly, the use of these observers allows the estimation of any number of faults, regardless of the number of measured outputs, and it can estimate additive and multiplicative faults. The observer gains can be solved together with the Lyapunov inequality using LMI-based computations and do not require to change the system model into a special form or the resolution of a system of partial differential equations like in (Stamnes, Aamo, & Kaasa, 2011).(Reformuler c'est incompréhensible)

In this paper, an active fault-tolerant control strategy is considered. Trajectory tracking of a quadrotor in the presence of actuator faults is studied.

References

Avram, Remus, Xiaodong Zhang and Jonathan Muse. "Nonlinear Adaptive Fault-Tolerant Quadrotor Altitude and Attitude Tracking With Multiple Actuator Faults." *IEEE Transactions on Control Systems Technology* (2018): 701–707.

Besancon, G. "Parameter/fault estimation in nonlinear systems and adaptive observers." *In Nonlinear Observers and Applications* (2007): 211-222.

Bouadi, H, M Bouchoucha and M Tadjine. "Modelling and stabilizing control laws design based on backstepping for an UAV type-quadrotor." *IFAC Proceedings Volumes* 40 (2007): 245-250.

Boyd, S, L El Ghaoui and E Feron. "Linear Matrix Inequalities in System and Control Theory." *Philadelphia: Society for Industrial Mathematics* (1997).

Cho, Young Man and Rajesh Raramani. "A Systematic Approach to Adaptive Observer Synthesis for Nonlinear Systems." *IEEE* (1995).

Corless, Martin and Jay Tu. "State and Input Estimation for a Class of Uncertain Systems." *Automatica* 34.6 (1998): 757-764.

Derafa, L, t Madani and A Benallegue. "Dynamic modelling and experimental identification of four rotor helicopter parameters." *ICIT Mumbai, India* (2006).

Ekramian, M, F Sheikholeslam and S Hosseinnia, M.J. "Adaptive state observer for Lipschitz nonlinear systems." *Systems & Control Letters* 62.4 (2013): 319-323.

Farza, M, et al. "Adaptive observers for nonlinearly parameterized class of nonlinear systems." *Automatica* 45.10 (2009): 2292-2299.

Floquet, T, C Edwards and S.K Spurgeon. "On Sliding Mode Observers for Systems with Unknown Inputs." *International Journal of Adaptive Control and Signal Processing* (2007): 638–656.

Freddi, A, S Longhi and A Monteriù. "Actuator fault detection system for a mini-quadrotor." *IEEE International Symposium on Industrial Electronics* (2010): 2055-2060.

Gao, C and G Duan. "Robust adaptive fault estimation for a class of nonlinear systems subject to multiplicative faults." *Circuits, Systems, and Signal Processing* 31.6 (2012): 2035-2046.

Grant , M, S Boyd and Y Ye. *Cvx: Matlab software for disciplined convex programming*. January 2020. 27 04 2023. <http://cvxr.com/cvx/>.

Hasanshahi, Mahsa, Aliakbar Ahmadi and Roya Amjadifard. "Robust Fault Tolerant Position Tracking Control for a Quadrotor UAV in Presence of Actuator Faults." *Proceedings of the 2019 6th International Conference on Control, Instrumentation and Automation (ICCIA)* (2019): 1-6.

Hong-Jun , Ma, et al. "Nonlinear High-Gain Observer-Based Diagnosis and Compensation for Actuator and Sensor Faults in a Quadrotor Unmanned Aerial Vehicle." *IEEE Transactions on Industrial Informatics* 15 (2019): 550-562.

Jain, Tushar , Joseph J. Yamé and Dominique Sauter. *Active Fault-Tolerant Control Systems-A Behavioral System Theoretic Perspective*. Springer Cham, 2018.

Jiang, B and F.N Chowdhury. "Parameter fault detection and estimation of a class of nonlinear systems using observers." *J. of the Franklin Institute* 342.7 (2005): 725-736.

Jiang, Jin and Xiang Yu. "Fault-tolerant control systems: A comparative study between active and passive approaches." *Annual Reviews in Control* (2012): 60-72.

Khalil, H. *Nonlinear Systems*. Prentice Hall, Upper Saddle River, NJ07458, 2002.

Khebbache, H, B Sait and F Yacef. "Robust Fault Tolerant Control With Sensor Faults for a Four Rotor Helicopter." *International Journal of Advances in Engineering & Technology* 3 (2012): 1-13.

Lien, Yu-Hsuan, Peng Chao-Chung and Chen Yi-Hsuan . "Adaptive Observer-Based Fault Detection and Fault-Tolerant Control of Quadrotors under Rotor Failure Conditions." *Applied Sciences* (2020): 3503.

Ouadine , Ahmed Youssef , et al. "UAV Quadrotor Fault Detection and Isolation Using Artificial Neural Network and Hammerstein-Wiener Model." *Studies in Informatics and Control* (2020).

Oucief, Nabil , Mohamed Tadjine and Salim Labiod . "A new methodology for an adaptive state observer design for a class of nonlinear systems with unknown parameters in unmeasured state dynamics." *ransactions of the Institute of Measurement and Control* 40.4 (2016): 1297-1308.

Oucief, Nabil, Mohamed Tadjine and Salim Labiod. "Adaptive observer-based fault estimation for a class of Lipschitz nonlinear systems." *Archives of Control Sciences* 26.2 (245–259).

Raoufi , Reza, Horacio Jose Marquez and Alan Solo. "$\mathcal{H}\infty$ sliding mode observers for uncertain nonlinear Lipschitz systems with fault estimation synthesis." *International Journal of Robust and Nonlinear Control* 20 (2010).

Shahriari-Kahkeshi, M, F Sheikholeslam and J Askari. "Adaptive fault detection and estimation scheme for a class of uncertain nonlinear systems." *Nonlinear Dynamics* 79.4 (2015): 2623-2637.

Stamnes, FFL N, O M Aamo and G-O Kaasa. "Redesign of adaptive observers for improved parameter identification in nonlinear systems." *Automatica* 47.2 (2011): 403-410.

That , Long Ton and Zhengtao Ding. "ADAPTIVE LIPSCHITZ OBSERVER DESIGN FOR A MAMMALIAN MODEL." *Asian Journal of Control* 16.2 (2014): 335–344.

Xiao-Lu, Ren. "Observer Design for Actuator Failure of a Quadrotor." *IEEE Access* 8 (2020): 152742-152750.

Xulin, Liu and Guo Yuying. "Fault tolerant control of a quadrotor UAV using control allocation." *Proceedings of the 2018 Chinese Control And Decision Conference (CCDC)* (2018): 1818-1824.

Yujiang , Zhong, et al. "Robust Actuator Fault Detection and Diagnosis for a Quadrotor UAV With External Disturbances." *IEEE Access* 6 (2018): 48169-48180.

Zhong, Yu-jiang, Zhixiang Liu and Youmi Zhang. "Active fault-tolerant tracking control of a quadrotor with model uncertainties and actuator faults." *Frontiers of Information Technology & Electronic Engineering* 20 (2019): 95-106.